Int. J. Heat Mass Transfer. Vol. 24, No. 5, pp. 851–857, 1981
Printed in Great Britain

0017–9310/81/050851–07 $02.00/0

HEAT TRANSFER AT AN UPSTREAM-FACING SURFACE WASHED BY FLUID *EN ROUTE* TO AN APERTURE IN THE SURFACE

E. M. SPARROW and U. GURDAL
Department of Mechanical Engineering,
University of Minnesota, Minneapolis, MN 55455, U.S.A.

(*Received* 29 *August* 1980 *and in revised form* 27 *October* 1980)

Abstract—Forced convection heat transfer coefficients were measured at a plane surface pierced by an aperture (or tube inlet) of diameter d into which fluid flows from a large upstream space. Heat transfer effects were confined to a portion of the surface contained within an annulus of outer diameter D which surrounds the aperture. The experiments were carried out for several values of the d/D ratio ranging from 1/6 to 1/14.4, and for each fixed d/D the Reynolds number was varied parametrically over a range that spanned a factor of five. Dimensional analysis led to a Reynolds number Re involving the rate of mass flow through the aperture and the outer diameter D of the thermally active region. The end result of the dimensional analysis indicated that for a fixed Prandtl number, the Nusselt number could depend on both Re and d/D. When the Nusselt number data for all cases were brought together on a single graph which spanned more than a decade in Reynolds number, no dependence on d/D was observed. The data are very well correlated by the equation $Nu = 2.88\, Re^{0.452}\, Pr^{1/3}$ over the range from $Re = 200$ to 3000. It was also found that the average rate of heat transfer per unit area drops off sharply as the outer diameter of the thermally active annular region increases.

NOMENCLATURE

A,	mass transfer area;
D,	outer diameter of active transfer annulus;
$\mathscr{D}$,	napthalene–air diffusion coefficient;
d,	aperture diameter;
K,	mass transfer coefficient, $\dot{m}/(\rho_{nw} - \rho_{n\infty})$;
ΔM,	change in mass during data run;
$\dot{m}$,	average rate of mass transfer per unit area;
Nu,	Nusselt number;
Pr,	Prandtl number;
Re,	Reynolds number, $\dot{w}/\mu D$;
Sh,	Sherwood number, $KD/\mathscr{D}$;
Sc,	Schmidt number, $\nu/\mathscr{D}$;
Δt,	duration of data run;
$\dot{w}$,	rate of fluid flow into aperture;
μ,	viscosity;
ν,	kinematic viscosity;
ρ,	density;
ρ_{nw},	napthalene vapor density at wall;
$\rho_{n\infty}$,	napthalene vapor density in free stream.

INTRODUCTION

THERE are many physical situations where an upstream-facing surface is washed by a fluid which flows into an aperture in the surface. As the fluid passes over the surface *en route* to the aperture, heat will be transferred if there is a temperature difference between the fluid and the surface. Such a flow occurs, for example, when a fluid is drawn from a large plenum chamber and enters a tube through an aperture in the wall of the plenum. A further and specific example of this type of flow is encountered in the making of fiberglass threads. There, the individual threads are formed as the molten glass passes through an aperture in the bottom wall of a containment vessel.

A schematic diagram of the aforementioned physical situation is presented in Fig. 1. As shown, fluid from a large upstream space passes into a circular aperture in a surface. The velocity vectors appearing in the figure are intended to portray the sink-like nature of the flow. Adjacent to the wall, the flow is of the boundary-layer type. Owing to the fact that the fluid accelerates rapidly as it approaches the aperture, it can be expected that the boundary layer will grow thinner as the aperture is approached. Correspondingly, the highest heat transfer coefficients are expected to occur along those portions of the wall that are closest to the aperture.

The objective of the present investigation is to

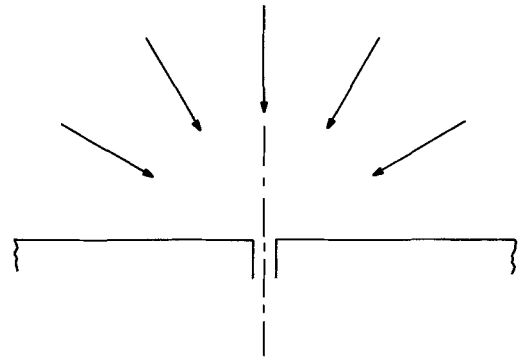

FIG. 1. Schematic diagram of an upstream-facing surface which is washed by fluid en route to an aperture in the surface.

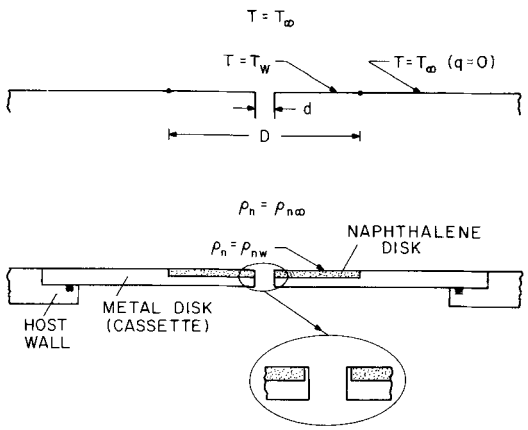

FIG. 2. Thermal conceptualization of the problem (upper diagram) and mass transfer setup actually used in the experiments (lower diagram).

determine heat transfer coefficients at the upstream-facing surface. To this end, experiments have been carried out using a test setup which closely resembles the physical situation shown in Fig. 1. As pictured in the figure, the upstream-facing surface extends out indefinitely, which is meant to imply that the aperture diameter is very small compared with a characteristic dimension of the surface. This feature was incorporated into the experimental apparatus.

The thermal boundary conditions of the experiments are depicted in the upper diagram of Fig. 2. As shown there, the aperture is surrounded by an annular region of diameter D where the surface temperature takes on a uniform value T_w. Beyond the diameter D, the surface temperature is equal to the ambient temperature T_∞, so that no heat transfer takes place.

The experiments were designed so that the diameter D of the thermally active region would be large compared with the aperture diameter d. This design condition was selected with a view to obtaining results that are independent of the d/D ratio, and this characteristic will be re-examined when the results are presented and discussed. The active-zone diameter D was varied parametrically during the course of the experiments, whereas the aperture diameter was held fixed.

The heat transfer coefficients, rather than being determined by direct thermal measurements, were obtained by applying the analogy between heat and mass transfer to measured mass transfer coefficients. The mass transfer measurements were made by means of the naphthalene sublimation technique. Compared to thermal measurements, the naphthalene technique offers the advantages of higher accuracy, near non-existence of extraneous losses, and better control of boundary conditions.

An experimental mass transfer arrangement which yields boundary conditions which are analogous to those for the aforementioned heat transfer problem is pictured in the lower diagram of Fig. 2. As seen there, an annular disk of solid naphthalene is contained in a larger metal disk such that the exposed surface of the naphthalene is continuous with that of the metal disk. The naphthalene sublimes, and the sublimation is driven by the difference between the naphthalene vapor concentration at the surface and that in the free stream, respectively ρ_{nw} and $\rho_{n\infty}$ ($\rho_{n\infty} = 0$ in the present experiments). This concentration difference is analogous to the temperature difference $(T_w - T_\infty)$ in the corresponding heat transfer problem. At the metal surface which frames the naphthalene, $\rho_n = 0$ and there is no mass transfer. This corresponds to the no-temperature difference, adiabatic portion of the surface for the thermal problem being modeled.

The experimental program was subdivided into four sets of data runs, with each set being characterized by a fixed value of the active-zone diameter D. At each such fixed D value, 10–12 data runs were made at a succession of Reynolds numbers. For the experiments as a whole, the Reynolds number was varied over an order of magnitude.

From the search of the literature, it appears that there is no published information that relates directly to the problem at hand. The most closely related work deals with the case of the abrupt contraction in a pipe. In Ede, Hislop and Morris [1], experiments are reported for water flow in a piping system for which there is a two-to-one contraction (on the diameter). Heat transfer coefficients were measured only in the region downstream of the contraction. The analytical work for the abrupt contraction appears to be confined to laminar flow [2, 3] and, here again, the only reported heat transfer results are for the tube which is situated downstream of the contraction.

THE EXPERIMENTS

Experimental apparatus

The upper wall of a large rectangular plenum chamber served as the host surface for the naphthalene test plate and its framing metal disk. The wall was a 61 × 61 cm (2 × 2 ft) square aluminum plate, 1.27 cm ($\frac{1}{2}$ in) thick. A circular opening fitted with a lap was machined concentric with the centerline of the square plate to accommodate the metal disk. This arrangement is illustrated in the lower diagram of Fig. 2. As seen there, the recess for the lap was made to precisely accommodate the thickness of the disk. An O-ring provided positive sealing between the disk and the lap, and screws entering from below (but not penetrating the upper surface of the disk) served to effect the seal. Continuity between the upstream-facing surfaces of the host wall and the disk was ensured by post-assembly machine sanding followed by painstaking hand polishing.

The metal disk which houses and frames the naphthalene test plate will hereafter be referred to as the cassette. The general outline of the cassette can be seen in the lower diagram of Fig. 2. It is an aluminum disk, 13.97 cm (5.5 in) in diameter and 0.508 cm (0.2 in)

thick. The disk is recessed to a depth that is slightly less than half its thickness in order to form an annular cavity for housing the solid naphthalene test plate (created by a casting process to be described shortly). The outer boundary of the naphthalene annulus is at diameter D. For the first set of data runs, D was machined to be 1.905 cm (0.750 in). Then, when those runs were completed, D was enlarged to a value of 2.540 cm (1.000 in) for the second set of runs. Further successive enlargements to attain D values of 3.810 and 4.572 cm (1.5 and 1.8 in) were made for the third and fourth sets of data runs.

The inner boundary of the annular cavity is the outer surface of a thin-wall sleeve whose bore serves as the aperture through which fluid passes from the upstream space into the plenum. The wall thickness of the sleeve is 0.0254 cm (0.010 in), and the bore diameter is 0.3175 cm (0.125 in).

With regard to the sleeve, its purpose was to avoid the situation where the naphthalene bounds the aperture. Had that situation prevailed, the aperture opening would have enlarged and become bell-mouthed during the course of a data run because of the high mass transfer coefficients that occur in that region. The sleeve, whose wall was made as thin as possible consistent with strength and life considerations, served to maintain a square-edged aperture of fixed diameter during each data run.

The plenum chamber, whose top wall is the host for the cassette, is an airtight steel enclosure. It is fitted with side-wall access ports, one of which was employed to facilitate the installation and removal of the cassette, respectively prior to and subsequent to a data run. A pipe stub which emanates from the base of the plenum enabled rapid connection or disconnection of a flexible vinyl hose which leads successively to a calibrated rotameter, a control valve, and a blower.

Operation of the apparatus was in the suction mode. Air from the temperature-controlled laboratory room is drawn in through the aperture. The air traverses the 1.2 m (4 ft) long plenum and exits via the base, from which point it passes through the rotameter, valve, and blower. From the blower, the air is ducted to a service corridor adjacent to the laboratory and then to an exhaust outside the building. The outside exhaust ensures that the air drawn toward the test surface is free of naphthalene vapor.

Downstream positioning of the blower was adopted to avoid preheating of the airflow. This precaution ensured that the temperature of the air passing over the naphthalene surface was always the same as the temperature of the air in the room.

With regard to instrumentation, the key instrument is a Sartorius analytical balance with a smallest scale reading of 0.1 mg and a maximum capacity of 200 g. To accommodate the 200 g maximum, shallow holes were machined into the underside of the cassette in order to remove excess mass. As will be described shortly, the balance was used to measure the mass of the cassette, including the naphthalene, both before and after a data run. The temperature of the air passing over the test surface was sensed by an ASTM-certified thermometer scribed at 0.1°F intervals. The accuracy of the thermometer was validated by comparisons with a secondary standard. For the mass flow measurements, a 2.5-cfm rotameter, previously calibrated by the volume-displacement method, was used. The pressure at the rotameter was measured with a water manometer in conjunction with a mercury barometer located in the laboratory.

Naphthalene test surfaces

The naphthalene test surface is fabricated by a casting process, using a two-part mold. One part of the mold is the cassette itself, and the other part is a thick, highly polished stainless steel plate. To initiate the casting procedure, the naphthalene remaining in the cassette from a prior data run is removed (by melting and subsequent evaporation). The empty cassette is then placed on the thick steel plate with the open face of the annular cavity downward. Then, molten naphthalene is poured into the cavity through access apertures in the rear face of the cassette. These apertures also enable escape of the air which is displaced by the molten napththalene.

Once the cavity has been filled and the naphthalene has solidified and cooled, the cassette is separated from the stainless steel plate. The naphthalene surface exposed by the separation is equal in smoothness to that of the plate against which it had solidified. A new naphthalene surface was fabricated for each data run using reagent-grade naphthalene.

Once the casting procedure had been completed, the cassette was brought to the laboratory room, at which time the naphthalene surface was covered with a glass plate. The cassette was then left to attain thermal equilibrium with the temperature-controlled air in the room.

Experimental procedure

To prepare for a data run, the blower was activated and the room lighting turned on about an hour before the intended start of the run. This enabled the blower to attain steady-state operation at the desired flow rate and also allowed for stabilization of any temperature disturbances caused by the presence of the additional heat sources (blower, lights and the experimenter). During this period, the cassette was positioned atop the upper wall of the plenum, to the side of the center hole in the wall, and the naphthalene surface was covered by the protective glass plate. The coupling between the rotameter and the base of the plenum was left unconnected, so that air was not drawn through the plenum.

Just prior to the data run, the glass cover was removed and the cassette (including the naphthalene) was weighed with the Sartorius analytical balance, at which time the cover was replaced. The cassette was then implanted in the upper wall of the plenum and the fastening screws, which seal the O-ring were tightened

(with access being gained through the side port of the plenum). The port cover was then sealed. Then, the protective cover was removed from the cassette and, with a virtually simultaneous motion, the plastic tube which couples the plenum and the rotameter was connected. Since the blower was already running, the start-up transient was confined to the time required to activate airflow through the plenum.

During the course of the run, the temperature, pressure, and flow rate were read periodically.

The duration of the data run was selected so that the mean recession of the naphthalene surface would not exceed 0.0038 cm (0.0015 in). The sublimation rate depends on the velocity of the airflow and on the naphthalene vapor pressure (which, in turn, depends on the temperature). At the typical temperatures of the experiments (~21°C, 70°F), the data-run durations ranged from 45 to 90 min, depending on the air velocity and the outer diameter D of the active mass transfer region. The change of mass during a run was in the range of 10–30 mg, again depending on the diameter D and on the velocity.

To conclude a data run, the plastic intercoupling to the rotameter was disconnected from the base of the plenum and, simultaneously, the protective glass cover was placed over the naphthalene. The plenum access port was then opened, and the cassette removed and subsequently weighed.

RESULTS AND DISCUSSION

The dimensionless parameters used to report the results will first be considered, followed by the presentation and discussion of the results.

Presentation parameters

An average mass transfer coefficient K was evaluated for each data run. If ΔM, Δt and A denote the net mass transfer for the data run, the duration time of the run, and the naphthalene surface area exposed to the airflow, respectively, then the rate of mass transfer per unit surface area follows as

$$\dot{m} = \Delta M/A\Delta t. \tag{1}$$

The mass transfer is driven by the difference between the density of the naphthalene vapor at the plate surface and that in the free stream, respectively, ρ_{nw} and $\rho_{n\infty}$. As noted in the Introduction, this density difference plays a role in the mass transfer process that is analogous to that played by the wall-to-stream temperature difference in the corresponding heat transfer problem. Thus, the mass transfer coefficient is defined as

$$K = \dot{m}/(\rho_{nw} - \rho_{n\infty}). \tag{2}$$

The vapour density ρ_{nw} was evaluated under the assumption that the solid naphthalene surface is in equilibrium with its subliming vapor. With the measured temperature as input, the naphthalene vapor pressure p_{nw} was obtained from the Sogin vapor pressure temperature relation [4]. Then, with p_{nw} and the temperature serving as inputs, ρ_{nw} was calculated from the perfect gas law (the molecular weight of naphthalene is 128.2). With regard to $\rho_{n\infty}$, it has already been noted that the flow approaching the test surface is devoid of naphthalene vapor, so that $\rho_{n\infty} = 0$. Thus, K is determined as the ratio of $\dot{m}$ to ρ_{nw}.

In seeking a correlation of the measured mass transfer coefficients, consideration was given to the parameters on which the coefficients are expected to depend. With regard to the influence of the fluid flow, a characteristic velocity is not readily identifiable. However, the rate $\dot{w}$ at which fluid flows into the aperture is, from the standpoint of applications, both readily identifiable and measurable (in effect, $\dot{w}$ represents the strength of the mass sink). Therefore, $\dot{w}$ will be used to characterize the fluid flow field.

The expected parametric dependence for the mass transfer coefficient then follows as

$$K = f(\dot{w}, D, d, \mathscr{D}, \rho, \mu). \tag{3}$$

The dimensions D and d respectively represent the outer diameter of the active mass transfer annulus and the diameter of the aperture. Another dimension which might also have been included in equation (3) is the overall size of the upstream-facing surface (e.g. the side or the diagonal of the 61 × 61 cm (2 × 2 ft) square plate). However, for the experiments, this dimension was very large compared with either D or d and may, therefore, be regarded as infinite.

The quantities $\mathscr{D}$, ρ and μ which appear in equation (3) are thermophysical properties. Among these, $\mathscr{D}$ is the naphthalene–air diffusion coefficient, and ρ and μ are the density and viscosity of the mixture of air and naphthalene vapor. Since the mass fraction of the naphthalene vapor in the mixture is minute (~0.0003), ρ and μ can be evaluated for pure air.

The application of dimensional analysis to equation (3) yields

$$KD/\mathscr{D} = f(\dot{w}/\mu D, \quad \nu/\mathscr{D}, d/D). \tag{4}$$

From the standard definitions of the Sherwood number and Schmidt number

$$Sh = KD/\mathscr{D}, \quad Sc = \nu/\mathscr{D} \tag{5}$$

where it may be noted that Sh and Sc are the mass

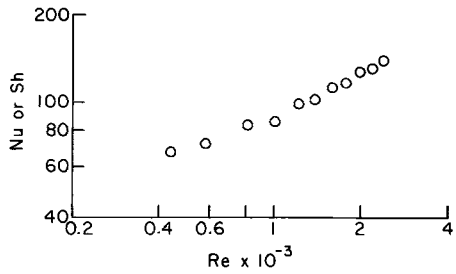

FIG. 3. Sherwood number (or Nusselt number) variation with Reynolds number for $d/D = \frac{1}{6}$.

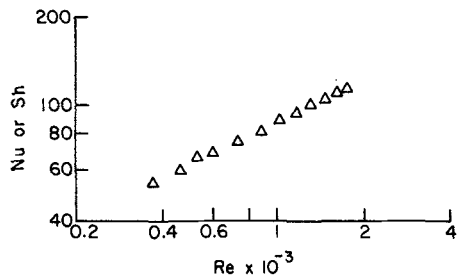

FIG. 4. Sherwood number (or Nusselt number) variation with Reynolds number for $d/D = \frac{1}{8}$.

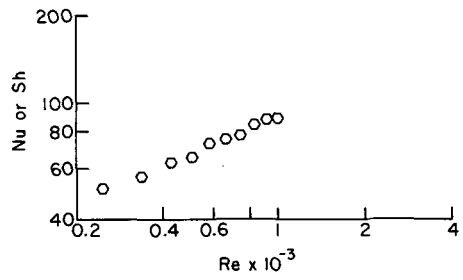

FIG. 6. Sherwood number (or Nusselt number) variation with Reynolds number for $d/D = \frac{1}{14.4}$.

transfer counterparts of the Nusselt and Prandtl numbers [5]. Also, the group $\dot{w}/\mu D$ plays the role of a Reynolds number, so we define

$$Re = \dot{w}/\mu D. \tag{6}$$

With these, equation (4) becomes

$$Sh = f(Re, Sc, d/D). \tag{7}$$

For the experiments, the Schmidt number is a constant equal to 2.5, so that the nature of the Schmidt number dependence indicated in equation (7) cannot be extracted from these experiments. Later, the experimental results will be generalized by incorporating a factor to take account of the effect of the Schmidt number.

As noted earlier, the experiments were designed with very small values of d/D with the aim of eliminating d/D as a parameter in the results. The role of d/D will be examined shortly. It may also be noted that in accordance with the analogy between heat and mass transfer, it follows that [5]

$$Nu = f(Re, Pr, d/D) \tag{8}$$

where the function f is the same for the two transfer processes. The present mass transfer results are analogous to heat transfer results for the thermal boundary conditions depicted in the upper diagram of Fig. 2. In view of the analogy, the phrases *heat transfer* and *mass transfer* will be used interchangeably in the forthcoming presentation of results.

Heat/mass transfer results

As was noted earlier, four sets of data runs were made, each for a fixed value of d/D. The respective values of d/D for these sets are $\frac{1}{6}$, $\frac{1}{8}$, $\frac{1}{12}$, and $\frac{1}{14.4}$. For a fixed d/D, equations (7) and (8) suggest that the data for Sh (or Nu) be plotted as a function of Re, and such plots are presented in Figs. 3–6. The successive figures correspond to decreasing d/D (i.e. increasing D at fixed d). The Reynolds numbers of the various figures span a range that is about a factor of five, but there is a shift toward lower Re with decreasing d/D in accordance with the fact that D appears in the denominator of the Reynolds number [equation (6)]. There is, however, substantial overlap in the Reynolds number ranges, and this will enable comparisons of the data for the various d/D.

Examination of Figs. 3–6 shows that the Sherwood (or Nusselt) number increases regularly with the Reynolds number. In particular, aside from localized deviations at the low Reynolds numbers, the data appearing in the respective figures lie on a straight line. In all cases, the slopes of the lines are approximately the same – yielding a Sh, Re or a Nu, Re power-law relation with an exponent just under one half.

The aforementioned regularity of the data for the various d/D encourages their being brought together in a single graph, and this has been done in Fig. 7. The

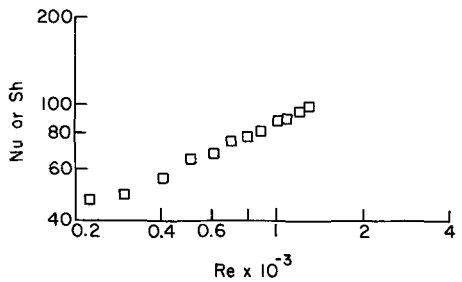

FIG. 5. Sherwood number (or Nusselt number) variation with Reynolds number for $d/D = \frac{1}{12}$.

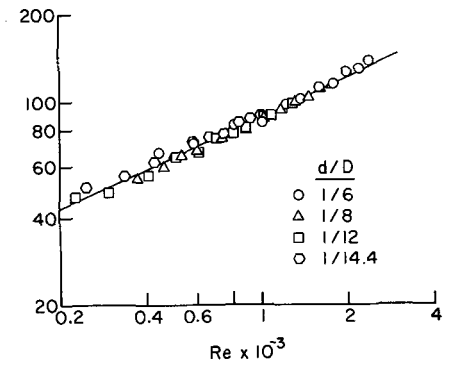

FIG. 7. Assemblage of Sh (Nu) vs Re data for all the d/D values of the experiment.

thus-assembled data span a range of Reynolds numbers that is slightly greater than an order of magnitude. From the figure, it can be seen that the data for all the d/D fall together, thereby indicating a correlation of the form

$$Sh = f(Re) \tag{9}$$

which is independent of d/D for $d/D \leq \frac{1}{6}$. The correlation might well apply for larger d/D values, but $d/D = \frac{1}{6}$ is the largest of the present experiments and, therefore, it represents the limit where definitive statements about the absence of the d/D effects can be made.

A least-squares straight line was fit to the data of Fig. 7, yielding

$$Sh = 3.91\,Re^{0.452} \quad \text{or} \quad Nu = 3.91\,Re^{0.452}. \tag{10}$$

This equation is recommended for application in the range $200 \leq Re \leq 3000$. Since the experiments underlying equation (10) correspond to $Sc = 2.5$, the equation is strictly applicable only for $Sc = Pr = 2.5$. To extend the generality of equation (1) to heat transfer situations where $Pr \neq 2.5$, the equation may be rephrased in the form

$$Nu = C\,Re^{0.452}\,Pr^{m} \tag{11}$$

where $C = 3.91/(2.5)^m$. It is conventional to take $m = \frac{1}{3}$ for external flows, and such a selection will be made here. With this, equation (11) becomes

$$Nu = 2.88\,Re^{0.452}\,Pr^{1/3}. \tag{12}$$

The correlation equation (10) facilitates the identification of trends in the mass transfer as a function of the air flow rate $\dot{w}$ and of the diameter D of the region of transfer. These same trends also apply to heat transfer. For this discussion, the difference between the 0.452 power and the $\frac{1}{2}$ power will be neglected. Consider first the average rate of mass transfer $\dot{m}$ per unit area which has already been defined by equation (1) (note that $\dot{m}$ corresponds to the average transfer rate over the active surface area A).

At a fixed concentration difference, equation (10) shows that

$$\dot{m} \sim D^{-3/2}, \quad \dot{w} \text{ fixed} \tag{13a}$$

$$\dot{m} \sim \dot{w}^{1/2}, \quad D \text{ fixed}. \tag{13b}$$

Thus, the average rate of mass transfer per unit area drops off very rapidly with the diameter of the active region. This indicates that the local mass fluxes at surface locations relatively remote from the aperture are very small compared with those at locations near the aperture. This finding is not unexpected in view of the rapid dropoff of the velocity with distance from the aperture (the potential flow model suggests an inverse square dropoff). Equation (13b) indicates that $\dot{m}$ increases with the half power of the flow rate, which is quite consistent with prior experience with laminar impingement-type flows.

With regard to the overall mass transfer rate $\dot{M} = \Delta M/\Delta t$ for an annular region of outer diameter D, equation (10) indicates that

$$\dot{M} \sim D^{1/2}, \quad \dot{w} \text{ fixed} \tag{14a}$$

$$\dot{M} \sim \dot{w}^{1/2}, \quad D \text{ fixed}. \tag{14b}$$

Equation (14a) shows that the overall rate of mass transfer increases as the diameter of the active zone increases, but to a power that is less than linear with the diameter and much less than D^2, which reflects the increase in surface area. The overall mass transfer rate depends on the half power of the rate of fluid flow through the aperture, as did the average mass transfer rate per unit area.

CONCLUDING REMARKS

Forced convection heat transfer characteristics have been determined for an upstream-facing surface which is washed by fluid *en route* to an aperture in the surface. The aperture, of diameter d, functions as a sink of mass with respect to the fluid in the upstream space. It is positioned centrally in a relatively large upstream-facing surface, with heat transfer effects confined to an annular region of outer diameter D which surrounds the aperture.

Experiments were performed for four parametric values of the diameter ratio d/D, which ranges from $\frac{1}{6}$ (largest value) to $\frac{1}{14.4}$ (smallest value). For each d/D, the Reynolds number was varied by approximately a factor of five.

Dimensional analysis led to a Reynolds number definition involving the rate of fluid flow through the aperture and the diameter D of the thermally active annulus. The end result of the dimensional analysis indicated that the Nusselt number could depend on the Reynolds number, the Prandtl number, and on the d/D ratio.

The experimental data for each specific d/D ratio, when plotted logarithmically as Nu vs Re, fell on a straight line with a slope slightly less than one half. When the Nusselt number data for all cases were plotted on a single graph which spanned more than a decade in Reynolds number, no dependence on d/D was observed. The insensitivity of the results to d/D is thus established for $d/D \leq \frac{1}{6}$ (the largest value investigated here). When a Prandtl-number scaling is incorporated, the present results are well represented by $Nu = 2.88\,Re^{0.452}\,Pr^{1/3}$ for $200 \leq Re \leq 3000$.

The experimental results also showed that the average rate of mass transfer per unit area decreases sharply as the diameter of the active region increases. This further suggests a sharp dropoff in the local mass flux with increasing distance from the aperture. The overall rate of mass transfer from an annular region of outer diameter D increases with the half power of D, which is much less than proportional to the increase in the transfer surface area with D. For an active zone of fixed dimensions, the rate of mass transfer increases with the square root of the rate of fluid flow through the annulus.

No information was found in the literature with

which to compare the present results.

Acknowledgement—The research reported here was performed under the auspices of the National Science Foundation.

REFERENCES

1. A. J. Ede, C. I. Hislop, and R. Morris, The effect on the local heat transfer coefficient in a pipe of an abrupt disturbance of the fluid flow: abrupt convergence and divergence of diameter ratio 2/1, *Chartered Mech. Engr* **3**, 312–314 (1956).
2. F. W. Schmidt and K. Wimmer, Laminar heat transfer in tubes with step change in cross section, pp. 19–28 in *Heat Transfer in Low Reynolds Number Flow* (edited by G. A. Brown and J. R. Moszynski) American Society of Mechanical Engineers. New York (1972).
3. E. B. Christiansen and S. J. Kelsey, Nonisothermal laminar contracted flow, *A.I.Ch.E. Jl* **3**, 713–720 (1972).
4. H. H. Sogin, Sublimation from disks to air streams flowing normal to their surfaces, *Trans. Am Soc. Mech. Engrs* **80**, 61–71 (1958).
5. E. R. G. Eckert, Analogies to heat transfer processes in *Measurements in Heat Transfer*. Hemisphere, Washington (1976).

TRANSFERT THERMIQUE A UNE SURFACE BALAYEE PAR UN FLUIDE SORTANT D'UNE OUVERTURE PRATIQUEE SUR CETTE SURFACE

Résumé—On mesure les coefficients de transfert thermique sur une surface percée d'une ouverture (ou tube d'entrée) de diamètre d, par laquelle un fluide s'écoule depuis un grand espace en amont. Les effets du transfert thermique sont confinés à une portion de la surface contenue dans un anneau de diamètre extérieur D qui entoure l'ouverture. Les expériences sont conduites pour plusieurs valeurs de d/D entre 1/6 et 1/14, 4 et pour chaque valeur le nombre de Reynolds varie dans un rapport de 1 à 5. L'analyse dimentionnelle conduit à un nombre de Reynolds basé sur le débit massique à travers l'ouverture et le diamètre D de la région thermiquement active. On montre que, pour un nombre de Prandtl fixé, le nombre de Nusselt peut dépendre à la fois de Re et de d/D. Quand on reporte toutes les valeurs de Nu sur un seul graphe qui correspond à une décade du nombre de Reynolds, on n'observe pas de dépendance vis-à-vis de d/D. Les mesures sont très bien représentées par la formule $Nu = 2{,}88\,Re^{0{,}452}\,Pr^{1/3}$ dans le domaine $Re = 200$ à 3000. On trouve aussi que le flux moyen de chaleur par unité de surface diminue rapidement quand le diamètre extérieur de la région annulaire thermiquement active augmente.

WÄRMEÜBERGANG AN EINER GEGEN DIE STRÖMUNG GERICHTETEN FLÄCHE, DIE VON EINEM FLUID IN RICHTUNG EINER ÖFFNUNG IN DIESER FLÄCHE UMSTRÖMT WIRD

Zusammenfassung — Es wurden Wärmeübergangskoeffizienten bei erzwungener Konvektion an einer ebenen Platte mit einer Öffnung (oder einem Rohreinlaß) vom Durchmesser d gemessen. In diese Öffnung strömt Flüssigkeit aus einem ausgedehnten, stromaufwärts gelegenen Gebeit. Wärmeübergangseffekte wurden in dem Teil der Oberfläche untersucht, welcher innerhalb eines Ringraums vom Außendurchmesser D die Öffnung umgibt. Die Experimente wurden für verschiedene Werte des Verhältnisses d/D im Bereich von 1/6 bis 1/14,4 ausgeführt. Für jedes feste Verhältnis d/D wurde die Reynolds-Zahl parametrisch in einem Bereich mit dem Faktor 5 variiert. Die Dimensionsanalyse führte zu einer Reynolds-Zahl, welche mit dem Massenstrom durch die Öffnung und dem Außendurchmesser D der thermisch aktiven Region gebildet wird. Das Endergebnis der Dimensionsanalyse zeigte, daß für eine feste Prandtl-Zahl die Nusselt-Zahl sowohl von Re als auch von d/D abhängig sein kann. Wenn man die Nusselt-Zahlen aller Fälle in ein einziges Diagramm einträgt, das mehr als eine Dekade der Reynolds-Zahl umfaßt, erkennt man jedoch keine Abhängigkeit von d/D. Die Werte ließen sich im Bereich von $Re = 200$ bis 3000 sehr gut nach der Gleichung $Nu = 2{,}88Re^{0{,}452}\,Pr^{1/3}$ korrelieren. Es wurde außerdem gefunden, daß die mittlere Wärmeübergangszahl scharf mit ansteigendem Außendurchmesser des thermisch aktiven Ringraumes abfällt.

ТЕПЛООБМЕН ПОВЕРХНОСТИ, ОРИЕНТИРОВАННОЙ ПРОТИВ ПОТОКА И ОМЫВАЕМОЙ ЖИДКОСТЬЮ, ДВИЖУЩЕЙСЯ ПО НАПРАВЛЕНИЮ К ОТВЕРСТИЮ В ПОВЕРХНОСТИ

Аннотация — Коэффициенты теплообмена вынужденной конвекцией измерены на плоской поверхности, имеющей отверстие (или вход в трубу) с диаметром d, в которое втекает жидкость из большого объёма, находящегося выше по потоку. Влияние теплообмена ограничено частью поверхности, заключённой в кольце с внешним диаметром D вокруг отверстия. Эксперименты выполнялись для нескольких значений соотношения d/D в диапазоне от 1/6 до 1/14,4, а для каждого d/D число Рейнольдса изменялось параметрически в интервале от Re до $5Re$. Из анализа размерностей получено число Рейнольдса Re, включающее скорость потока через отверстие и внешний диаметр D области влияния теплообмена. Конечный результат анализа размерностей указывает на то, что для заданного числа Прандтля число Нуссельта может зависеть как от Re, так и от d/D. Когда экспериментальные данные по числу Нуссельта были обобщены на едином графике, для более чем десяти значений числа Рейнольдса зависимости параметра от d/D не наблюдалось. Экспериментальные данные очень хорошо описываются уравнением $Nu = 2{,}88Re^{0{,}452}Pr^{1/3}$ в диапазоне чисел Рейнольдса от 200 до 3000. Было найдено также, что средняя интенсивность теплообмена на единицу площади резко падает с возрастанием внешнего диаметра кольцевой области D.